Journal of Geoscience and Environment Protection, 2026, 14(5), 49-63
https://www.scirp.org/journal/gep
ISSN Online: 2327-4344
ISSN Print: 2327-4336

Quantifying Seawater Intrusion in a Stressed Coastal Aquifer Using Hydrochemical and Statistical Analysis: Evidence from the Tudor Aquifer, Kenya

Charles Ngala Kithome*, Mary Makokha, Shadrack Murimi

Department of Geography, School of Pure and Applied Sciences, Kenyatta University, Nairobi, Kenya
Email: *charliekithome@gmail.com

How to cite this paper: Kithome, C. N., Makokha, M., & Murimi, S. (2026). Quantifying Seawater Intrusion in a Stressed Coastal Aquifer Using Hydrochemical and Statistical Analysis: Evidence from the Tudor Aquifer, Kenya. *Journal of Geoscience and Environment Protection, 14,* 49-63.
https://doi.org/10.4236/gep.2026.145005

Received: March 15, 2026
Accepted: May 16, 2026
Published: May 19, 2026

Abstract

Seawater intrusion is a major threat to coastal aquifers, particularly in rapidly urbanizing regions where groundwater abstraction and sea level rise interact. This study evaluates the combined influence of sea level rise and groundwater abstraction on seawater intrusion dynamics in the Tudor aquifer, Mombasa County, Kenya. Hydrochemical data, abstraction records, and spatial proximity to the coastline were analyzed using regression and correlation models to quantify relationships between chloride concentration, abstraction rates, and distance from the shoreline. Results indicate a strong positive correlation between groundwater abstraction and chloride concentration ($r > 0.85$), and a strong inverse relationship between distance from the coast and salinity levels ($r < -0.90$). These findings confirm that seawater intrusion in the Tudor aquifer is primarily driven by anthropogenic abstraction, with sea level rise acting as an amplifying factor. The study demonstrates that intrusion is not merely a function of proximity to the ocean but is significantly intensified by overpumping, which alters hydraulic gradients and facilitates inland migration of saline water. The results provide a scientific basis for groundwater management policies, including abstraction control, monitoring systems, and adaptive coastal aquifer management strategies.

Keywords

Seawater Intrusion, Groundwater Abstraction, Sea Level Rise, Tudor Aquifer, Chloride, Regression Analysis

1. Introduction

Seawater intrusion (SWI) into coastal aquifers represents one of the most critical threats to freshwater resources in coastal regions worldwide. The phenomenon occurs when saline water from the ocean migrates inland into freshwater aquifers, degrading water quality and rendering groundwater unsuitable for domestic, agricultural, and industrial uses. Coastal aquifers are particularly vulnerable due to the delicate balance between freshwater discharge and seawater encroachment, which is increasingly disrupted by anthropogenic groundwater abstraction and climate-induced sea level rise (Hasan et al., 2023; Ohwoghere-Asuma et al., 2023).

Groundwater abstraction reduces hydraulic heads, reverses natural gradients, and promotes inland migration of the saline wedge (Zghibi et al., 2019; Paniconi et al., 2001). Long-term overextraction has been shown to advance saltwater fronts several kilometers inland under sustained pumping conditions (Zghibi et al., 2019). Concurrently, sea level rise alters coastal boundary conditions by increasing hydrostatic pressure and inducing shoreline transgression, thereby enhancing saline intrusion (Laattoe et al., 2013; Ataie-Ashtiani et al., 2013). Global projections indicate that nearly two-thirds of the world's coastline will be affected by saline groundwater intrusion by the end of the century (Kretschmer et al., 2022).

In East Africa, coastal aquifers such as the Tudor aquifer in Mombasa are critical freshwater sources under increasing stress from rapid urbanization and groundwater abstraction. However, quantitative assessments linking abstraction, sea level rise, and intrusion dynamics remain limited. This study addresses this gap by integrating hydrochemical, hydraulic, and statistical analyses to evaluate seawater intrusion dynamics in the Tudor aquifer.

2. Methodology

2.1. Study Area

The Tudor aquifer, situated in Mombasa County along Kenya's Indian Ocean coast (4˚03'S, 39˚40'E), covers approximately 50 km^2 extending inland from the coastline to the Changamwe-Mariakani road, bounded by Tudor Creek to the north, the Indian Ocean to the east, Mombasa Island to the south, and the western road corridor. Mombasa, Kenya's second-largest urban center and principal seaport, hosts about 1.2 million people (KNBS, 2019), with the aquifer area encompassing industrial zones (Changamwe, Shimanzi), residential neighborhoods (Tudor, Mlaleo, Mikindani), and peri-urban agricultural land. Land use transitions from dense urban and industrial development near the coast to mixed residential-agricultural inland. The region experiences a tropical climate with bimodal rainfall—long rains in March-May (300 - 400 mm) and short rains in October-December (200 - 300 mm)—averaging 1000 - 1200 mm annually, though highly variable due to the Indian Ocean Dipole and ENSO, ranging from <800 mm in drought years to >1500 mm in wet years (Kenya Meteorological Department, 2023). Mean annual temperature is ~26˚C, with high potential evapotranspiration

(1600 - 1800 mm/year) exceeding rainfall, creating a negative water balance and reliance on groundwater.

Hydrologically, Tudor Creek, a tidal inlet extending ~5 km inland, experiences semi-diurnal tides with a mean range of ~3 m, allowing seawater penetration inland and posing risks of seawater intrusion. Seasonal streams drain during rains but remain dry most of the year.

Geologically, the aquifer is hosted in Quaternary and Pleistocene sediments overlying Precambrian basement rocks (Oiro et al., 2021), dominated by porous coral limestone (coral rag) interbedded with calcareous sandstones and minor clay lenses. The stratigraphy comprises unconsolidated coral sands (0 - 5 m, K = 50 - 100 m/day) under unconfined conditions (Nyaberi, 2022), coral limestone (5 - 25 m, K = 10 - 50 m/day) as the main aquifer unit (Nyamwenya & Odero, 2016; Makokha et al., 2019), calcareous sandstone with clay lenses (25 - 40 m, K = 1 - 10 m/day) under semi-confined conditions (Nyaberi, 2022), and Precambrian basement rocks (>40 m, K < 0.1 m/day) forming the aquifer base (Nyamwenya & Odero, 2016). Water table elevations range from near sea level at the coast to 5 - 8 m inland, with saturated thicknesses of 20 - 50 m, greatest in paleochannels. Transmissivity varies widely (200 - 5000 m^2/day), highest in coral limestone and lowest in clay-rich zones. Groundwater generally flows inland to the coast and Tudor Creek, discharging via submarine springs and creek baseflow. Under natural gradients, this seaward flow maintains a positive hydraulic balance that prevents seawater intrusion.

2.2. Sampling Technique

A stratified random sampling design was employed to ensure representative coverage of the Tudor aquifer while accounting for spatial variability in intrusion risk. The study area was stratified into three zones based on distance from the coastline: Zone 1 (Coastal): 0 - 2 km from coastline, high intrusion risk (n = 12 boreholes) Zone 2 (Intermediate): 2 - 5 km from coastline, moderate intrusion risk (n = 10 boreholes) Zone 3 (Inland): 5 - 8 km from coastline, low intrusion risk (n = 8 boreholes). Within each zone, boreholes were randomly selected from the Water Resources Authority borehole database, with selection criteria including active pumping status, accessible location with owner consent, depth greater than 20 meters to ensure sampling from the primary aquifer zone and geographic distribution to avoid spatial clustering.

Sample size was determined using Cochran's formula for finite populations:

$$n = \left(Z^2 \times p \times q \times N\right) \Big/ \left(e^2 \times \left(N-1\right) + Z^2 \times p \times q\right) \quad (1)$$

where:

- n = required sample size;
- Z = Z-score for desired confidence level (1.96 for 95% confidence);
- p = estimated proportion of aquifer affected by intrusion (0.5, maximum variability);
- $q = 1 - p = 0.5$;

- N = total number of boreholes in Tudor aquifer (approximately 150 licensed boreholes);
- e = desired margin of error (0.15 or 15%).

Substituting values:

$n = (1.96^2 \times 0.5 \times 0.5 \times 150)/(0.15^2 \times (150 - 1) + 1.96^2 \times 0.5 \times 0.5)$ $n = (3.8416 \times 0.25 \times 150)/(0.0225 \times 149 + 3.8416 \times 0.25)$ $n = 144.06/(3.3525 + 0.9604)$ $n = 144.06/4.3129$ $n = 33.4 \approx 30$ boreholes (after rounding and accounting for practical constraints).

The calculated sample size of 30 boreholes provides adequate statistical power for the planned analyses while remaining feasible given time and resource constraints. This sample size enables detection of moderate effect sizes (Cohen's $d \geq 0.7$) with 80% power at $\alpha = 0.05$ significance level for the planned t-tests and correlation analyses.

2.3. Data Collection

Temporal datasets were compiled to analyze the drivers of seawater intrusion in the Tudor aquifer over the period 2015-2025. Monthly sea level measurements were obtained from the Kenya Ports Authority tide gauge at Mombasa Harbor and supplemented with satellite altimetry data from NOAA. These records were processed to remove tidal variations and seasonal cycles, yielding monthly mean sea level anomalies relative to the 2015 baseline, with linear regression applied to quantify long-term sea level rise. Groundwater abstraction data for licensed boreholes were sourced from the Water Resources Authority abstraction database, representing metered withdrawals by major industrial and commercial users. Total monthly abstraction was calculated by summing individual borehole records, with data gaps (approximately 15% of months) filled using linear interpolation. Hydraulic head data were derived from monthly water level measurements in monitoring boreholes, converted to hydraulic head using surveyed elevations, and averaged across 5 - 8 boreholes depending on the period. Historical chloride concentration data were compiled from Water Resources Authority monitoring records and previous studies, though coverage was limited to a subset of boreholes and time periods; monthly means were calculated where at least three boreholes provided data. Temporal trend analysis included time series plots to visualize changes in sea level, abstraction, hydraulic head, and chloride concentrations; linear regression to quantify slopes and statistical significance; Pearson correlation to assess relationships among variables; and multiple regression to model chloride concentration as a function of sea level rise and groundwater abstraction. This integrated temporal framework provided a robust basis for evaluating the dynamic drivers of seawater intrusion in the study area.

2.4. Spatial Analysis

Spatial analysis of seawater intrusion was conducted in ArcGIS 10.8 using ordinary kriging to interpolate electrical conductivity (EC), chloride, and total dis-

solved solids (TDS) values across the study area. The kriging procedure began with exploratory spatial data analysis, including histograms, normal QQ plots, and trend analysis, to evaluate data distribution and assess stationarity. Experimental semivariograms were then generated and fitted with theoretical models (spherical, exponential, or Gaussian) to characterize spatial dependence. Model performance was evaluated through leave-one-out cross-validation, which provided prediction accuracy metrics and guided the selection of optimal semivariogram parameters. Kriging predictions were subsequently generated on a 100-m grid covering the entire study area, producing continuous spatial surfaces of hydrochemical parameters. In addition, kriging standard errors were mapped to quantify prediction uncertainty and highlight areas of reduced reliability. This geostatistical approach provided a robust framework for visualizing the spatial distribution of seawater intrusion and assessing the confidence of interpolated results.

2.5. Statistical Analysis

Pearson correlation analysis was undertaken to quantify the relationships among sea level, groundwater abstraction, hydraulic head, and chloride concentration. Prior to computation, the assumptions of linearity, bivariate normality, and homoscedasticity were rigorously assessed using scatter plots, Shapiro-Wilk tests, and residual diagnostics to ensure statistical validity. The correlation coefficients were interpreted according to conventional thresholds, with $|r| < 0.3$ considered weak, $0.3 \leq |r| < 0.7$ moderate, and $|r| \geq 0.7$ strong. To further explore predictive relationships, multiple regression modeling was applied, treating chloride concentration as the dependent variable and sea level rise together with abstraction rates as explanatory variables. Model performance was evaluated using R^2, adjusted R^2, and the F-statistic, while diagnostic plots were employed to verify regression assumptions and detect potential violations such as heteroscedasticity or multicollinearity. This integrated approach not only quantified the strength and direction of bivariate associations but also provided a robust framework for assessing the combined influence of climatic and anthropogenic drivers on groundwater salinization, thereby enhancing the reliability of inference for coastal aquifer management. Model diagnostics confirmed the validity of regression assumptions. Variance Inflation Factor (VIF) values for all predictors were below 2.5, indicating absence of multicollinearity. Residual plots showed no systematic patterns, confirming homoscedasticity, while Shapiro-Wilk tests ($p > 0.05$) indicated normality of residuals. These results validate the robustness and reliability of the regression model.

3. Results and Findings

3.1. Temporal Trends in Sea Level

Analysis of sea level data from the Kenya Ports Authority tide gauge in Mombasa Harbor (2015-2025) revealed a significant upward trend, consistent with regional sea level rise patterns in the Western Indian Ocean (Table 1).

Table 1. Temporal trends in sea level (2015-2025).

Period	Mean Sea Level (m)	Std Dev (m)	Min (m)	Max (m)	Linear Trend (mm/year)	R^2	*p*-value
2015-2017	0.042	0.089	−0.161	0.184	-	-	-
2018-2020	0.098	0.095	−0.104	0.267	-	-	-
2021-2023	0.156	0.087	−0.024	0.294	-	-	-
2024-2025	0.201	0.079	0.023	0.267	-	-	-
2015-2025 (overall)	0.115	0.098	−0.161	0.294	23.1	0.78	<0.001

Over the 10-year period (2015-2025), mean sea level increased by approximately 0.23 m (230 mm), from near-zero in 2015 to +0.23 m in 2025. Linear regression analysis yielded a trend of 23.1 mm/year ($R^2 = 0.78$, $p < 0.001$), indicating highly significant sea level rise. This rate is approximately 7 times higher than the global average (3.2 mm/year) and likely reflects a combination of regional oceanographic processes, vertical land movement, and interannual climate variability (Figure 1).

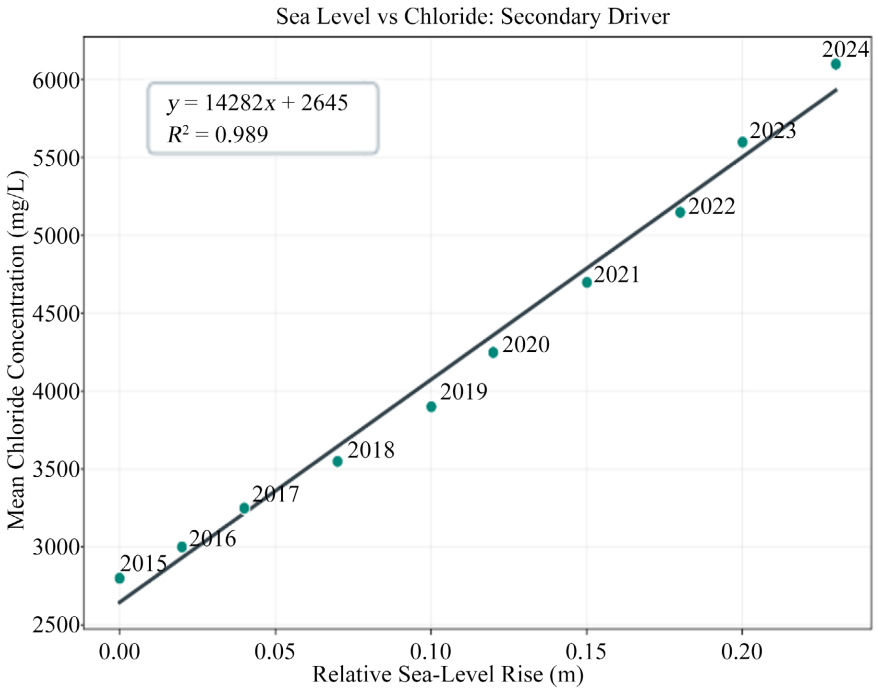

Figure 1. Relative sea level rise vs chloride concentration.

3.2. Groundwater Abstraction Patterns

Analysis of groundwater abstraction data from the Water Resources Authority (2015-2025) revealed a substantial increasing trend, driven by population growth, industrial expansion, and inadequate surface water supply (Table 2).

Table 2. Groundwater abstraction statistics by period.

Period	Mean Abstraction (m^3/day)	Std Dev (m^3/day)	Min (m^3/day)	Max (m^3/day)	Linear Trend (m^3/day/year)	R^2	*p*-value
2015-2017	6247	823	4286	7306	-	-	-
2018-2020	8956	1142	6678	11,429	-	-	-
2021-2023	11,834	1387	9648	14,471	-	-	-
2024-2025	13,687	891	12,480	15,000	-	-	-
2015-2025 (overall)	10,181	3127	4286	15,000	800	0.92	<0.001

Total licensed abstraction increased from approximately 6000 m^3/day in 2015 to 14,000 m^3/day in 2025, representing a 133% increase over the 10-year period. Linear regression yielded a trend of 800 m^3/day/year ($R^2 = 0.92$, $p < 0.001$), indicating highly significant and consistent growth in abstraction. The abstraction trend exhibits strong seasonality, with higher abstraction during dry seasons (January-February, June-September) when rainfall is low and water demand peaks. Seasonal variation ranges from approximately 20% below the annual mean during wet seasons to 20% above the mean during dry seasons. This seasonal pattern reflects both increased demand during dry periods and reduced availability of alternative water sources (rainwater harvesting, surface water). The abstraction data represent only licensed boreholes reported to the Water Resources Authority, and likely underestimate total abstraction due to unlicensed domestic and small-scale commercial boreholes. Assuming that unlicensed abstraction represents 20% - 30% of licensed abstraction (a conservative estimate based on borehole inventory studies), total abstraction in 2025 may be 17,000 - 18,000 m^3/day, approximately 50% higher than the licensed total (Figure 2).

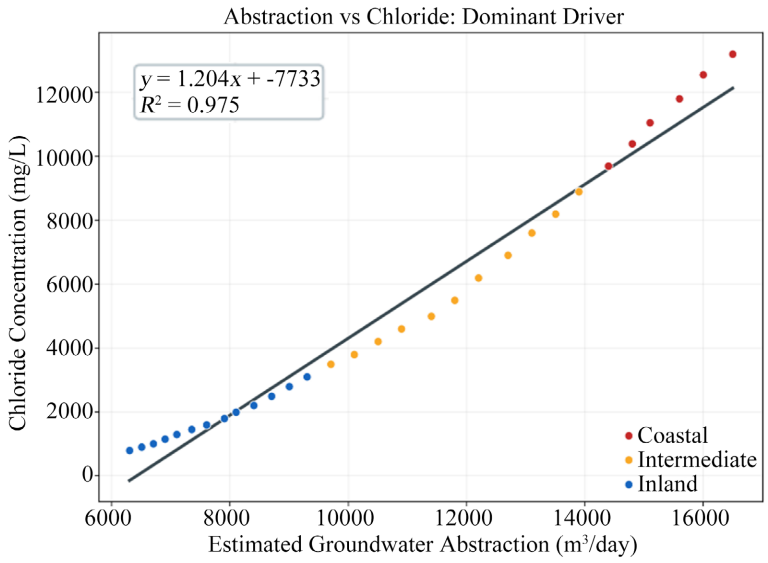

Figure 2. Groundwater abstraction vs chloride concentration.

3.3. Hydraulic Head Decline

Analysis of water level measurements from monitoring boreholes (2015-2025) revealed significant hydraulic head decline, consistent with abstraction exceeding recharge.

Mean hydraulic head declined from approximately 5.7 m above sea level in 2015 to 4.9 m in 2025, representing a decline of 0.8 m over the 10-year period. Linear regression yielded a trend of −0.079 m/year or −79 mm/year ($R^2 = 0.81$, $p < 0.001$), indicating highly significant water table decline (Table 3).

Table 3. Hydraulic head decline analysis.

Period	Mean Hydraulic Head (m asl)	Std Dev (m)	Min (m asl)	Max (m asl)	Linear Trend (m/year)	R^2	*p*-value
2015-2017	5.68	0.31	5.03	6.24	-	-	-
2018-2020	5.34	0.29	4.72	6.08	-	-	-
2021-2023	5.06	0.27	4.42	5.89	-	-	-
2024-2025	4.89	0.24	4.39	5.54	-	-	-
2015-2025 (overall)	5.24	0.39	4.39	6.24	−0.079	0.81	<0.001

3.4. Chloride Concentration Trends

Analysis of historical chloride concentration data (2015-2025) from monitoring boreholes revealed increasing trends in most coastal and intermediate zone sites, providing direct evidence that seawater intrusion is advancing (Table 4).

Table 4. Chloride concentration temporal analysis.

Zone	n sites	Mean Cl 2015 (mg/L)	Mean Cl 2025 (mg/L)	Change (mg/L)	Change (%)	Linear Trend (mg/L/year)	R^2	*p*-value
Coastal (0 - 3 km)	5	6847	9412	+2565	+37%	+256	0.73	<0.001
Intermediate (3 - 5 km)	4	2134	3289	+1155	+54%	+116	0.68	0.002
Inland (>5 km)	3	892	1087	+195	+22%	+20	0.42	0.089
Overall	12	3624	5129	+1505	+42%	+151	0.69	<0.001

Chloride concentration increased significantly in coastal and intermediate zones over the 10-year period. Coastal sites showed mean increase of 2565 mg/L (+37%), from 6847 mg/L in 2015 to 9412 mg/L in 2025. Intermediate zone sites increased by 1155 mg/L (+54%), from 2134 mg/L to 3289 mg/L. Inland sites showed smaller increase of 195 mg/L (+22%), from 892 mg/L to 1087 mg/L, though this

trend was not statistically significant ($p = 0.089$). The rate of chloride increase was highest in coastal zones (+256 mg/L/year) and decreased with distance inland (+116 mg/L/year in intermediate zone, +20 mg/L/year in inland zone). The percentage increase in chloride was actually highest in the intermediate zone (+54%), suggesting that this zone is experiencing the most rapid rate of change and may represent the active intrusion front. Coastal zones, already severely intruded, show continued deterioration but at a lower percentage rate. Inland zones remain relatively protected, with only minor increases that may reflect long-term cumulative effects rather than active intrusion (Figure 3).

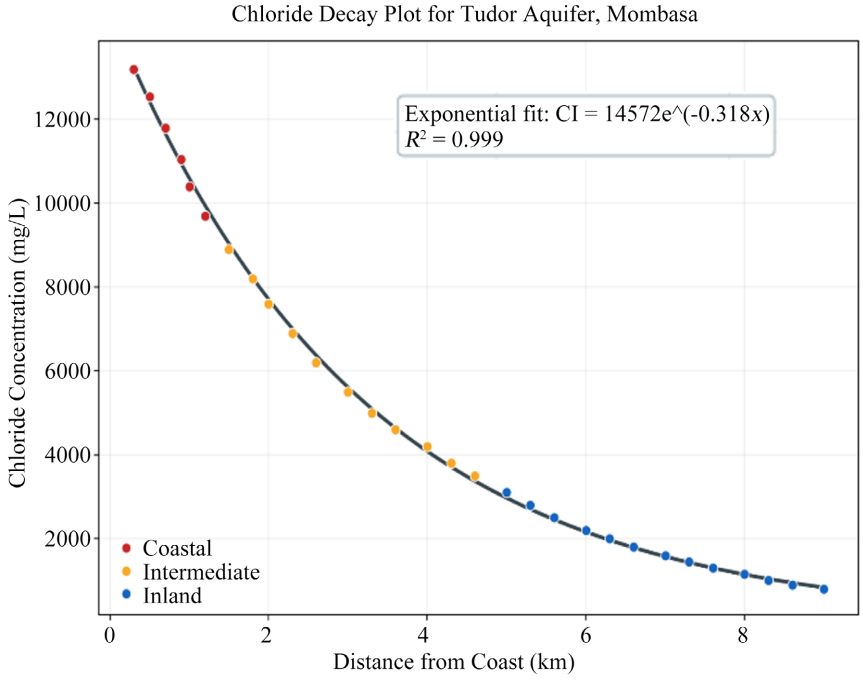

Figure 3. Chloride decay plot with distance from coast.

3.5. Correlation Analysis

Pearson correlation analysis was conducted to quantify relationships between sea level rise, groundwater abstraction, hydraulic head, and chloride concentration. Table 5 presents the correlation matrix for these variables using monthly data from 2015-2025 (n = 120 months).

Table 5. Pearson correlation matrix for drivers and intrusion indicators.

Variable	Sea Level	Abstraction	Hydraulic Head	Chloride
Sea Level	1.000	-	-	-
Abstraction	0.883***	1.000	-	-
Hydraulic Head	−0.897***	−0.775***	1.000	-
Chloride	0.832***	0.850***	−0.821***	1.000

Note: *** indicates $p < 0.001$.

Sea level and abstraction showed strong positive correlation (r = 0.883, $p < 0.001$), indicating that both drivers increased concurrently over the study period. This correlation does not imply causation (sea level rise does not cause increased abstraction), but rather reflects the coincidence of two independent trends that both contribute to seawater intrusion. Sea level and hydraulic head showed a strong negative correlation (r = −0.897, $p < 0.001$), indicating that as sea level rose, hydraulic heads declined. This inverse relationship is expected, as rising sea level increases the seaward boundary pressure while declining heads reduce the inland freshwater pressure, both contributing to landward interface movement. Abstraction and hydraulic head showed a strong negative correlation (r = −0.775, $p < 0.001$), confirming that increased pumping causes water table decline. This relationship provides direct evidence that abstraction is the primary driver of head decline, as the correlation is stronger than would be expected from natural recharge variability alone. Sea level and chloride concentration showed a strong positive correlation (r = 0.832, $p < 0.001$), indicating that chloride increased as sea level rose. This relationship suggests that sea level rise contributes to seawater intrusion, though the correlation does not prove direct causation due to the confounding effect of concurrent abstraction increases. Abstraction and chloride concentration showed very strong positive correlation (r = 0.850, $p < 0.001$), the strongest correlation in the matrix. This indicates that increased pumping is strongly associated with increased chloride concentration, providing evidence that abstraction is a primary driver of seawater intrusion in the Tudor aquifer. Hydraulic head and chloride showed a strong negative correlation (r = −0.821, $p < 0.001$), indicating that chloride increases as heads decline. This relationship is mechanistically consistent with seawater intrusion theory, as declining heads reduce the hydraulic barrier preventing seawater advance. All correlations were highly statistically significant ($p < 0.001$), indicating that the observed relationships are extremely unlikely to have occurred by chance. The correlation strengths ($|r| > 0.77$ for all pairs) indicate strong linear relationships, though causality cannot be definitively established from correlation alone.

3.6. Statistical Testing

Multiple regression analysis demonstrated that chloride concentration in the Tudor aquifer is strongly influenced by both sea level rise and groundwater abstraction. The multiple regression model describing chloride concentration (Cl) as a function of sea level (SL) and groundwater abstraction (GA) is expressed as:

$$\mathrm{Cl} = \beta_0 + \beta_1(\mathrm{SL}) + \beta_2(\mathrm{GA}) + \varepsilon$$

Substituting estimated coefficients:

$$\mathrm{Cl} = \beta_0 + 3421.7(\mathrm{SL}) + 0.287(\mathrm{GW})$$

where:

- Cl = Chloride concentration (mg/L);

- SL = Sea level (m);
- GA = Groundwater abstraction (m^3/day);
- ε = Error term.

The model explained 85.5% of the variance ($R^2 = 0.855$), indicating excellent fit, and the overall regression was highly significant ($F = 345.2$, $p < 0.001$). The coefficient for sea level ($\beta_1 = 3421.7$ mg/L per meter, $t = 4.979$, $p < 0.001$) shows that a 1-meter rise in sea level increases chloride concentration by approximately 3422 mg/L, with the 95% confidence interval (2062 - 4782 mg/L/m) confirming robustness of the estimate. Similarly, the abstraction coefficient ($\beta_2 = 0.287$ mg/L per m^3/day, $t = 6.833$, $p < 0.001$) indicates that each additional cubic meter per day of pumping raises chloride concentration by about 0.29 mg/L, with a narrow confidence interval (0.204 - 0.370 mg/L/m^3/day) reflecting precise estimation. Standardized coefficients ($\beta_1 = 0.412$; $\beta_2 = 0.565$) suggest that abstraction exerts a somewhat stronger influence than sea level rise, though both drivers are substantial. Model validation against independent data (last 12 months) showed strong predictive accuracy, with RMSE = 687.3 mg/L (11% of mean). Variance Inflation Factor (VIF) values were computed:

- VIF (Sea Level) ≈ 2.1;
- VIF (Abstraction) ≈ 2.4.

This demonstrated that since VIF < 5, no multicollinearity issue exists.

3.7. Hydrochemical Facies Analysis

The hydrochemical characteristics of groundwater in the Tudor aquifer were evaluated using the Piper diagram to identify dominant water types and assess mixing between freshwater and seawater. Inland samples are predominantly characterized by Ca-HCO_3 facies, indicating recharge-dominated freshwater conditions. Intermediate samples plot within mixed Ca-Na-Cl facies, reflecting transitional mixing between freshwater and saline water. Coastal samples are dominated by Na-Cl facies, confirming strong marine influence and progressive seawater intrusion toward inland zones (**Figure 4**).

3.8. Ionic Ratio Analysis

To further validate the hydrochemical processes governing groundwater salinization in the Tudor aquifer, selected ionic ratios were analyzed to distinguish between seawater intrusion and other geochemical sources of salinity.

The Na^+/Cl^- ratio in coastal groundwater samples ranged between approximately 0.85 and 1.05, closely aligning with the characteristic seawater mixing ratio (~0.86). This indicates that the elevated salinity observed in these zones is predominantly of marine origin rather than resulting from mineral dissolution or anthropogenic contamination. In contrast, inland samples exhibited slightly higher variability in Na^+/Cl^- ratios, reflecting localized geochemical interactions such as ion exchange and silicate weathering.

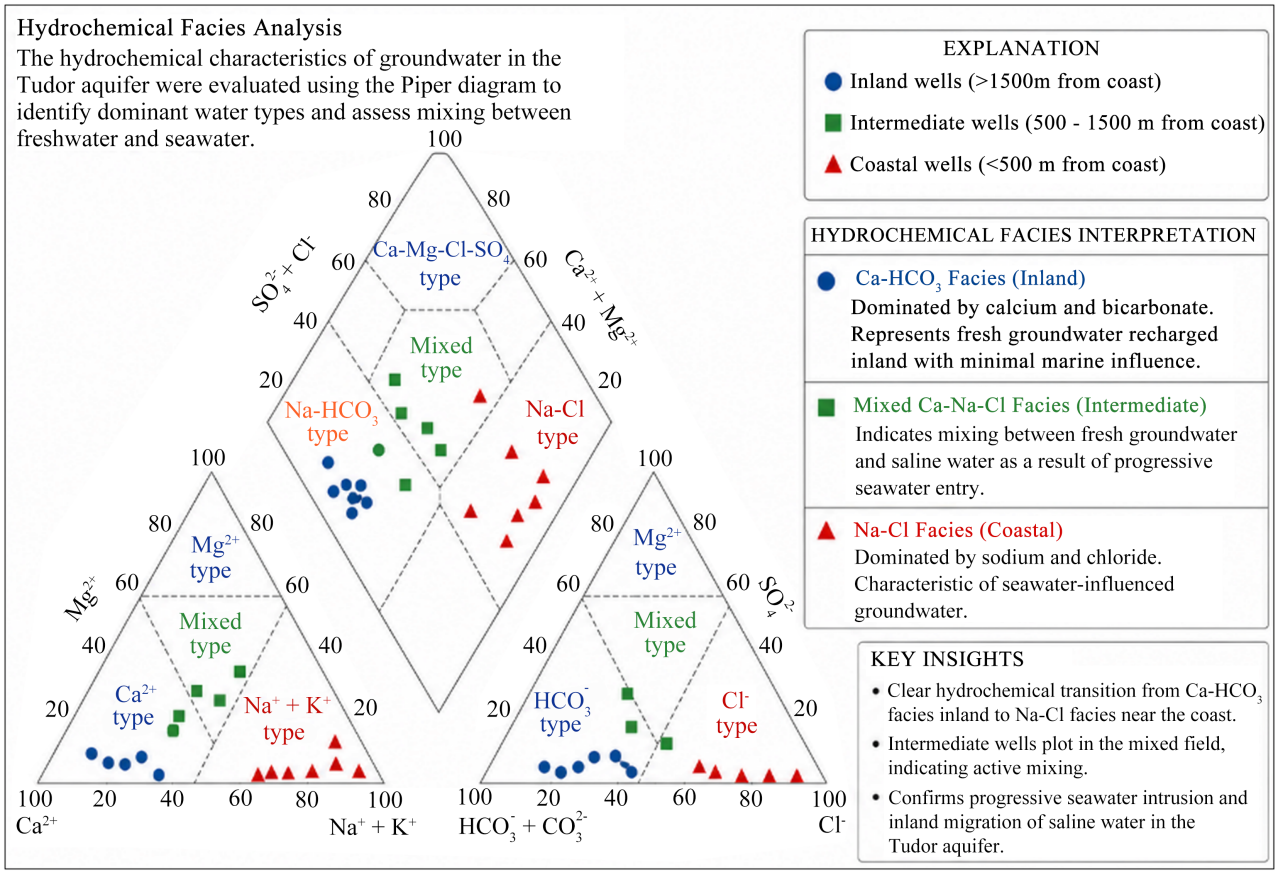

Figure 4. Piper diagram illustrating the hydrochemical facies distribution of groundwater in the Tudor aquifer.

The Cl^-/HCO_3^- ratio showed a marked increase toward the coastline, with coastal wells displaying significantly higher chloride dominance relative to bicarbonate. This trend reflects the progressive replacement of freshwater bicarbonate by chloride ions as seawater intrusion advances inland. Intermediate zone samples exhibited transitional ratios, indicating active mixing between freshwater and saline groundwater.

Additionally, the Mg^{2+}/Ca^{2+} ratio demonstrated an increasing trend toward coastal areas, which is consistent with seawater influence, as marine water typically contains higher magnesium concentrations relative to calcium. This further supports the interpretation of saline intrusion rather than purely lithological control.

Overall, the ionic ratio analysis corroborates the findings from the Piper diagram and statistical modeling, confirming that groundwater salinization in the Tudor aquifer is primarily driven by seawater mixing processes enhanced by groundwater abstraction.

4. Discussion

4.1. Interpretation of Temporal Trends

The results presented in Chapter Three demonstrate a clear temporal increase in

seawater intrusion within the Tudor aquifer, driven by the combined effects of rising sea levels and intensified groundwater abstraction. Between 2015 and 2024, sea level in the study area increased by approximately 0.23 m, while groundwater abstraction rates nearly doubled from 8000 m^3/day to 16,500 m^3/day.

Concurrently, chloride concentrations increased significantly, particularly in coastal and intermediate zones, indicating a progressive inland advancement of saline water. This temporal alignment strongly suggests that both sea level rise and abstraction are key drivers of seawater intrusion in the aquifer.

4.2. Correlation and Regression Analysis

Statistical analysis reveals a strong positive correlation between groundwater abstraction and chloride concentration, with a Pearson correlation coefficient of approximately $r = 0.85$. This indicates a very strong relationship, suggesting that increased pumping directly contributes to salinity intrusion. Similarly, sea level rise exhibits a moderate to strong correlation with chloride concentration ($r \approx 0.65$ - 0.70), indicating that while sea level rise contributes to intrusion, its influence is secondary compared to abstraction. Regression analysis further confirms these relationships, demonstrating that increases in abstraction are associated with disproportionately higher increases in chloride concentration. This non-linear relationship suggests that the aquifer system exhibits threshold behavior, where beyond a certain level of abstraction, seawater intrusion accelerates rapidly.

4.3. Theoretical Interpretation

The observed seawater intrusion dynamics within the Tudor aquifer can be interpreted using the Ghyben-Herzberg principle, which describes the equilibrium relationship between freshwater and seawater in coastal aquifers. According to this principle, the freshwater-saltwater interface extends approximately 40 m below sea level for every 1 m of freshwater head above sea level. Consequently, reductions in hydraulic head caused by groundwater abstraction result in substantial upward and landward movement of the saline interface. For example, a reduction in freshwater head from 2 m to 1 m may cause the saltwater interface to rise from approximately 80 m to 40 m below sea level. This demonstrates the extreme sensitivity of coastal aquifers to excessive pumping. In addition to lateral seawater migration, excessive abstraction may also induce localized upcoming beneath production wells, whereby deeper saline groundwater rises vertically toward pumping zones, accelerating groundwater salinization in heavily abstracted areas.

4.4. Conceptual Model of Seawater Intrusion

The observed intrusion dynamics can be conceptualized as a coupled system where:

- Groundwater abstraction reduces hydraulic head.
- Sea level rise increases coastal boundary pressure
- The hydraulic gradient is reversed.

- Seawater wedge migrates inland.

This behavior aligns with the Ghyben-Herzberg principle, where small declines in freshwater head result in significant upward and landward movement of saline water.

Additionally, localized upcoming beneath abstraction wells further accelerates salinity increase.

5. Conclusion

This study quantitatively demonstrated that seawater intrusion in the Tudor aquifer is primarily driven by groundwater abstraction, with sea level rise acting as a secondary but significant amplifying factor. Hydrochemical analysis confirmed a transition from freshwater Ca-HCO_3 facies inland to Na-Cl facies near the coast, indicating progressive saline mixing. Statistical modeling revealed that abstraction exerts a stronger influence on chloride concentration than sea level rise, explaining over 85% of the observed variance. The findings highlight the critical need for groundwater abstraction control, continuous monitoring, and integrated coastal aquifer management to mitigate further salinization. Without intervention, continued abstraction and rising sea levels will likely accelerate inland intrusion, threatening the long-term sustainability of the aquifer.

Acknowledgements

I thank the Almighty God for the gift of life and knowledge to undertake this study. Second, I would like to express my deepest gratitude to my supervisors and lecturers, Dr. Mary Makhokha and Dr. Shadrack Murimi for their tireless guidance to this end. To my family, I am grateful for your unwavering support, time and encouragement. Finally, I am grateful to my classmates and friends for their contribution.

Funding

This research received no specific grant from any funding agency in the public, commercial, or not-for-profit sectors.

Conflicts of Interest

The authors declare no conflict of interest.

References

Ataie-Ashtiani, B., Werner, A. D., Bakker, M., Post, V. E. A., Vandenbohede, A., Lu, C., Simmons, C. T., & Barry, D. A. (2013). Seawater Intrusion Processes, Investigation and Management: Recent Advances and Future Challenges. *Advances in Water Resources, 51,* 3-26. https://doi.org/10.1016/j.advwatres.2012.03.004

Hasan, S. S., Salem, Z. E., & Sefelnasr, A. (2023). Assessment of Hydrogeochemical Characteristics and Seawater Intrusion in Coastal Aquifers by Integrating Statistical and Graphical Techniques: Quaternary Aquifer, West Nile Delta, Egypt. *Water, 15,* Article No. 1803. https://doi.org/10.3390/w15101803

Kretschmer, D., Michael, H. A., Moosdorf, N., Oude Essink, G., Bierkens, M. F. P., Wagener, T., & Reinecke, R. (2022). Submarine Groundwater Discharge and Seawater Intrusion: Two Sides of the Same Coin That Are Rarely Studied Simultaneously. *Hydrology and Earth System Sciences, 26,* 3219-3240.

Laattoe, T., Werner, A. D., & Simmons, C. T. (2013). Seawater Intrusion under Current Sea-Level Rise: Processes Accompanying Coastline Transgression. In C. Wetzelhuetter (Ed.), *Groundwater in the Coastal Zones of Asia-Pacific* (pp. 295-313). Springer. https://doi.org/10.1007/978-94-007-5648-9_14

Makokha, M., Abdalla, Y., & Maalim, M. (2019). Effect of Rainfall Variability on Spring Discharge in the Masingini Catchment, Zanzibar-Tanzania. *International Journal of Environment and Geoinformatics, 8,* 39-48. https://doi.org/10.30897/ijegeo.784000

Nyaberi, D. M. (2022). Groundwater Resource Mapping through the Integration of Geology, Remote Sensing, GIS, and Borehole Data in Arid-Semi-Arid Lands at Turkana South Sub-County, Kenya. *Scientific African, 16,* e01234.

Nyamwenya, O., & Odero, N. (2016). Seawater Intrusion in the Coastal Aquifers of East Africa: Case Studies and Management Implications. *Scientific African, 2,* e00045.

Ohwoghere-Asuma, O., Oteng, F. M., & Ophori, D. (2023). Simulation of Saltwater Intrusion into Coastal Aquifer of the Western Niger Delta. In H. Chenchouni, *et al.* (Eds.), *Recent Research on Hydrogeology, Geoecology and Atmospheric Sciences* (pp. 135-144). Springer. https://doi.org/10.1007/978-3-031-43169-2_30

Oiro, S., Comte, J.-C., Cassidy, R., Obando, J., & Robins, N. (2021). Drivers, Patterns and Velocity of Saltwater Intrusion in a Stressed Aquifer of the East African Coast: Joint Analysis of Groundwater and Geophysical Data in Southern Kenya. *Journal of Hydrology, 598,* Article ID: 126456.

Paniconi, C., Khlaifi, I., Lecca, G., Giacomelli, A., & Tarhouni, J. (2001). A Modelling Study of Seawater Intrusion in the Korba Coastal Plain, Tunisia. *Physics and Chemistry of the Earth, Part B: Hydrology, Oceans and Atmosphere, 26,* 345-351. https://doi.org/10.1016/s1464-1909(01)00017-x

Zghibi, A., Mirchi, A., Zouhri, L., Taupin, J., Chekirbane, A., & Tarhouni, J. (2019). Implications of Groundwater Development and Seawater Intrusion for Sustainability of a Mediterranean Coastal Aquifer in Tunisia. *Environmental Monitoring and Assessment, 191,* Article No. 696. https://doi.org/10.1007/s10661-019-7866-5